J Mater Sci (2008) 43:4309–4315
DOI 10.1007/s10853-008-2632-z

Toughness and microstructural analysis of superduplex stainless steel joined by plasma arc welding

Emel Taban

Received: 18 March 2008 / Accepted: 2 April 2008 / Published online: 17 April 2008

Abstract EN 1.4410 (UNS S32750) superduplex stainless steel (SDSS) with a thickness of 6.5 mm has been welded by plasma arc welding (PAW) process with different heat inputs. To determine the mechanical properties, impact toughness testing at subzero temperatures starting from −20 °C down to −60 °C was carried out while fractographs were examined by scanning electron microscopy (SEM). Microstructural examination included macro- and microphotographs of the cross sections, ferrite content measurements and hardness survey of the weld zones. Interpreting all data obtained, results were compared depending on the heat inputs of the joints while the relation between heat input and properties was explained. Promising low temperature toughness, results were obtained while it was concluded that the variation of the heat input influenced mainly the ferrite content and hardness of the weld zones. Results showed that PAW, which is considered immature process in welding of SDSS, can be employed for 1.4410 superduplex grade with controlled heat input so the properties.

Introduction

Duplex stainless steels (DSSs), approximately with 50% ferrite and 50% austenite at their room temperature microstructure, have been introduced in the 1970s; however, they have been evolved rapidly since 1980s. Significant improvements both in material design and weldability have been made leading DSS to range from the cost efficient lean grades to the high alloyed superduplex grades for more demanding applications. The distinction between duplex and superduplex is not standardized. The term of superduplex is usually associated with about 25% Cr, ≥3.5% Mo and >0.2% N providing an increased pitting resistance equivalent number (PRE_N) ≥40 [1–6]. Superduplex stainless steels (SDSSs) belong to the duplex family and they have increased levels of Cr, Mo and N than the standard duplex grades, resulting with a higher strength and improved corrosion resistance and resistance especially to stress corrosion cracking in H_2S containing aggressive mediums [7–9]. The superior corrosion resistance, strength and/or combination of both properties due to their strict composition control and microstructural balance have provided these stainless grades to be used in many applications, and they are often selected to substitute austenitic alloys where stress corrosion cracking and pitting corrosion are of concern such as in the oil and gas, paper and pulp, petrochemical industries and in power generation [1–4, 9, 10].

Properties of DSSs and weld metals are dependent on the phase balance and can be affected by secondary phases. For the common arc welding methods, using filler metals with increased nickel content and specified minimum heat input is standard practice [11]. The weldability of standard DSS grades both with conventional arc welding processes such as shielded metal arc welding (SMAW) [12–15], gas tungsten arc welding (GTAW) [16, 17], flux cored arc welding (FCAW) [14], submerged arc welding (SAW) [14] and with solid state processes such as flash butt resistance [18] welding has been reported by various researchers.

The practical application of any steel on a larger scale is critically dependent on its weldability for fabrication. Productivity is always a key issue in manufacturing, and as

E. Taban (✉)
Mechanical Engineering Department, Engineering Faculty, Kocaeli University, 41200 Kocaeli, Turkey
e-mail: emel.taban@yahoo.com; emelt@kocaeli.edu.tr; emel.taban@soete.ugent.be

the use and demand for DSSs have increased, weld productivity has become more important. In principle productivity can be improved by increasing weld speed or by decreasing the number of weld beads [11]. A number of studies on relatively novel processes of DSSs were reported such as electron beam welding [17, 19], laser welding [20] and hybrid process [11]. However, attention should be paid for autogeneous processes and in particular for beam welding processes associated with very rapid cooling, increasing the risk of unbalanced microstructure [11].

Duplex stainless steels have good weldability similar to austenitic grades with a comparable alloying content. Although higher alloying content of superduplex weld metals compared to the duplex grades provides improved properties, it is increasingly difficult to optimize welding thermal cycles when the alloying content is increased. SDSS grades are more sensitive to the variations in weld metal composition or welding parameters [5, 7]. The difficulty in welding is mainly to obtain austenite amounts close to 50% and to avoid the formation of deleterious intermetallic phases on cooling and reheating passes [8]. The ferrite/austenite ratio depends on the energy input in welding, since it controls the cooling rate and ferrite/austenite transformation. Cooling time has strong effects on the impact toughness that the ferrite content and microhardness decreases with the increasing of cooling time. Very low heat inputs lead to high ferrite contents and intense chromium nitride precipitation while high heat inputs and/or long exposure between 1,000 and 600 °C tend to produce coarse-grained weld deposits or cause precipitation of brittle phases like σ and χ. For these reasons, it is desirable to control welding parameters such that cooling is slow enough for adequate austenite formation but also fast enough to prevent deleterious precipitation [4, 8, 9, 11, 21, 22]. In general, depending on the thickness and joint type, SDSSs are recommended to be welded with heat inputs in the range of 0.5–2.0 kJ/mm [8]. Taking into account on some difficulties about SDSS welding and considering published research work, reported studies concentrated on welding of these steels are found to be relatively scarce compared to that of standard duplex grades. Concerning SDSS, SMAW and synergic cold wire submerged arc welding (SCW^{TM} SAW) was studied by Karlsson and Tolling [11] while SMAW and TIG welding was also reported by Comer and Looney [23]. As a novel process, friction stir welding of SDSS has been accomplished and reported by Sato et al. [24].

In plasma arc welding (PAW), the electric arc is generated between a non-consumable tungsten electrode and the constrained using a copper nozzle with a small opening at the tip. By forcing the plasma gas and arc through a constricted orifice, the torch delivers a high concentration of energy to a small area giving higher welding speeds and producing welds with high penetration/width ratios, thus limiting the heat affected zone (HAZ) dimensions. For these reasons PAW is a useful technique for welding austenitic steels and can be applied to SDSSs [25]. To increase the productivity, there is an interest in applying PAW process in recent years resulted with researches concerning PAW of standard 1.4462 duplex grade have been realised by Urena et al. and Sun et al. [25, 26]. However, no published study about plasma weldability or properties of superduplex grades has been determined up to now. Taking into account of the increasing interest in demands of using superduplex grades and plasma welding for industrial applications, this study is planned to focus on PAW of SDSS plates.

In this study, low temperature toughness and microstructural properties of plasma arc welded 1.4410 SDSS with different heat inputs were investigated, and differences between the results of the welds due to the heat input range were compared while microstructure–property relation was mentioned. And the possibility of PAW process applications which is relatively novel for SDSSs in industrial fields still obtaining an acceptable ferrite:austenite ratio was also investigated.

Material and experimental procedure

Superduplex stainless steel conforming to grades 1.4410 and X2CrNiMoN 25.6.3 in EN 10088 and EN 10028.7 and to UNS S32750 in ASTM A240 with a thickness of 6.5 mm has been used concerning present research. Chemical composition of the base metal (BM) is given in Table 1.

Plasma arc welding of 1.4410 superduplex grade was realised in industrial conditions in keyhole mode without filler metal and by DCEN polarity. Straight plate edges

Table 1 Chemical composition of the superduplex stainless steel base metal (data from chemical analysis by XRD and from the steel producer [27])

Chemical composition (wt.%)[a]												
C	Si	Mn	P	Cr	Cu	Ni	Mo	Ti	V	Nb	N	Co
0.025 [<0.030]	0.30	0.86	0.037	24.33 [25]	0.18	6.65 [6.5]	3.72 [3.6]	0.003	0.077	0.06	0.28 [0.26]	0.05

[a] Values between square brackets are obtained from the steel producer

perpendicular to the plate surface have been prepared while the weld pool was protected by a high purity Ar gas. One pass welding without preheat and with a heat input of 1.90 kJ/mm was used for the plasma arc Weld 1. Weld 2 of SDSS plates was produced with PAW with similar conditions and with a heat input of 2.25 kJ/mm which exceeds the upper limit of the recommended range [8, 27].

Each weld was mechanically tested using sub-sized notch impact test samples extracted transverse to the weld and prepared with notches positioned at the weld metal centre (WM), HAZ and BM. Since much welding technology associated with DSSs has been generated from offshore applications, significant emphasis is placed on the lower temperature properties of the WM and HAZ [14]; so impact testing was carried out at subzero temperatures such as −20, −40 and −60 °C. Examinations of the fractographs from both welds tested at −60 °C were carried out with a JEOL JSM 5600 SEM.

For microstructural investigations, cross sections of plasma arc welded SDSS joints were prepared, polished and etched electrolytically in NaOH solution. Macro- and microphotographs were obtained by light optical microscope (LOM) with 200× magnification at the BM, WM and HAZs of each weld. Ferrite content measurements of the welds in ferrite % were done with a Fischer Ferritscope across the weld zones. Microhardness measurements on each weld were carried out with a depth of 1.5 mm subsurface from the face and root sides and with 0.5 mm distance between each indentation.

Results and discussion

The mean notch impact values expressed in joule are shown in Fig. 1a and b, respectively, for Weld 1 and Weld 2.

Impact toughness of DSS welds is specified at design temperature or another specified temperature. Although the acceptance criteria vary significantly, examples of typical impact toughness requirements are a minimum of 34 J at −40 °C, 35 J average and 27 J minimum at −46 °C [5]. Depending on these criteria, it can easily be said that both joints pass the minimum requirements with much higher values such as 106 J and 102 J for WM and 72 and 82 J for HAZ, respectively, for Weld 1 and Weld 2 even at −60 °C. Fractographs from both welds tested at −60 °C with the notch position at weld metal, respectively, for Weld 1 and Weld 2, were examined with SEM (see Fig. 2). In accordance with the toughness test results, ductile fracture for both welds was observed since the figure reveals some fine dimples.

The microstructural examination on the specimens of both joints has been carried out using LOM and with 200× magnification. The investigation of the welds has been

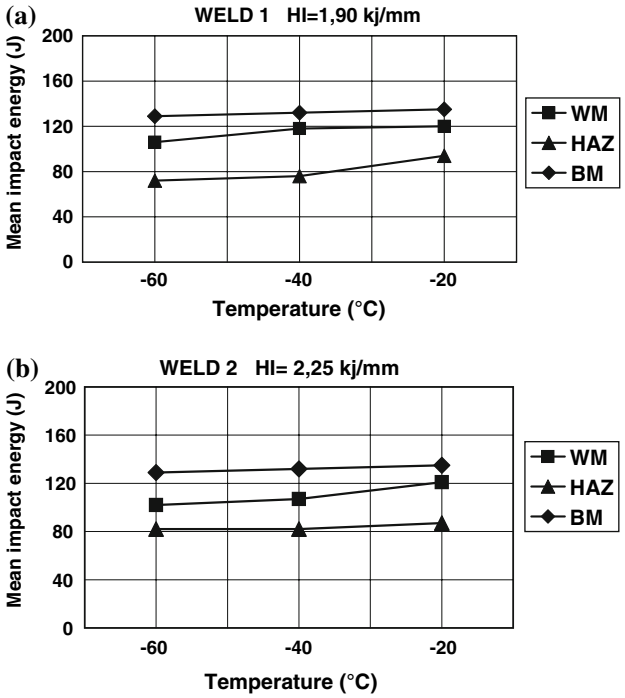

Fig. 1 Notch impact toughness graphs of plasma arc welds of SDSS: (**a**) Weld 1 and (**b**) Weld 2

performed from BM across HAZ to WM respectively. The macro- and microstructures of the related BM and weld zones are shown in Figs. 3 and 4, respectively, for Weld 1 and Weld 2.

The SDSS BM has shown an elongated grain structure, typical of that of a rolled product with ferrite and austenite duplex microstructure in accordance with the literature [1, 13]. Since the primary solidification phase is ferrite and given the fairly rapid cooling due to the weld thermal cycle, diffusional transformation to austenite can be suppressed on cooling to room temperature providing a predominantly ferritic structure at the fusion zone; the microstructure of a fusion weld of the DSSs can significantly differ from that in the BM compared to the martensitic and austenitic types. The HAZ is heated to temperatures close to the solidus, inducing transformation from the original two-phase microstructure to ferrite and this retains on cooling [28]. HAZ close to the weld metal is heated up to temperatures at which transformation to ferrite and even melting on the grain boundaries occur. Some grain coarsening together with denticulate austenitic dendrites at the grain boundaries exists in accordance with the literature [15]. In Figs. 3 and 4, a relatively narrow HAZ for Weld 1 and some grain growth affecting subsequent epitaxial growth of the columnar ferrite grains inside the fusion pool can be seen; similar to the study by Urena et al. [25], some secondary austenite mainly at the weld metals in the form of Widmanstatten needles growing into the

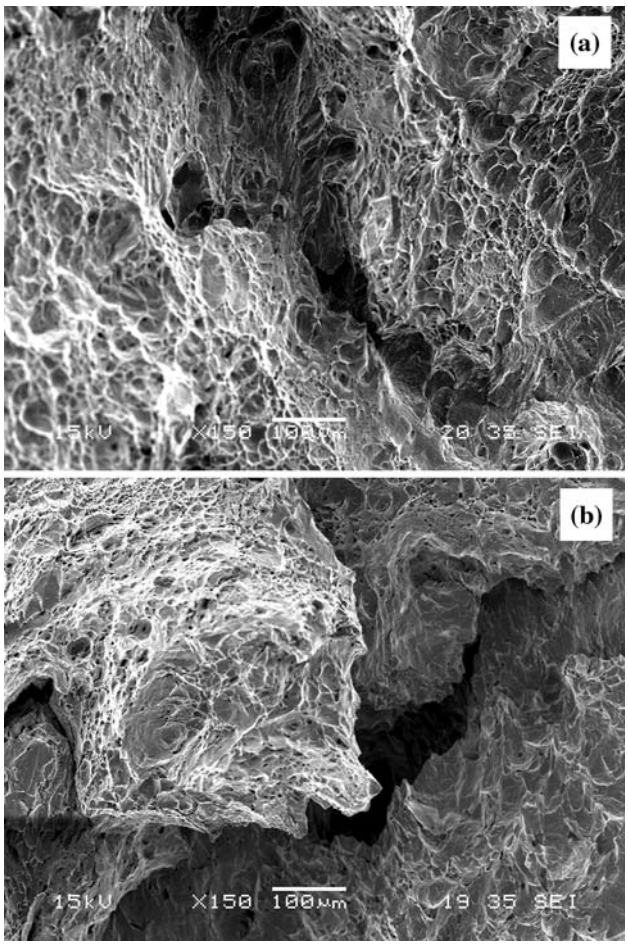

Fig. 2 Fractographs of samples from WM tested at −60° C (**a**) Weld 1 and (**b**) Weld 2

ferrite grains was observed similar to the literature [9, 18]. HAZ gets a little bit wider in Weld 2 than in Weld 1 due to the heat input range (see Figs. 3 and 4); and due to the heat input increase some grain coarsening of the ferrite grains was also observed in the micrographs of Weld 2.

WRC-1992 diagram allows ferrite prediction based on composition up to 100 FN [1]. Taking into account of this, Cr_{eq} and Ni_{eq} values of BM were calculated to predict the ferrite content of the fused metal. Chromium equivalent of approximately 28.1 and nickel equivalent of 13.2 for BM were calculated using chemical composition data. A FN of approximately 65 is obtained for the weld metal. Since a rough conversation from FN to volume percent for the duplex alloys is 70% [1], approximately 45.5% ferrite is predicted for the related weld due to the WRC diagram. Ferrite content data obtained with a Fischer Ferritscope on the macrosections of the joints with the measurements across the BM left, left part of the HAZ, weld metal, right part of the HAZ and BM right, which are given in Table 2. Ferrite % data also includes the values obtained from the face, middle and root parts of the related positions.

Depending on the results obtained from the Ferritscope measurements, weld metal ferrite content of approximately 48.9% and 44.4% were obtained, respectively, for Weld 1 and Weld 2. The effect of the heat input is not considered in WRC diagram however; the measured ferrite content values are close to the predicted ones calculated by WRC-1992 diagram as mentioned above. For ensuring the excellent combination of properties of DSS, it is essential to maintain a ferrite/austenite ratio close to 50:50. However, the phase balance is upset during welding due to the rapid cooling. This can result in weld metal ferrite contents much in excess of 50%. In order to maintain the original chemical and physical properties of the as-received duplex BM, the phase balance of the weld metal and the HAZ is critical [26]. Weld metal shall fulfil a Ferrite Number (FN) requirement of FN = 30–70 (approximately 22–70%) in TIG weldments. With other processes and at locations exposed to the corrosive environment and/or possible hydrogen cracking, ferrite content of the weld metal of approximately 22–60% may be required [3], but usually 30–70% range is acceptable for practical applications [8, 25, 26]. In accordance with the literature, WM ferrite content values measured between 48.9% and 44.4% for the plasma arc Welds 1 and 2, respectively, conforms to acceptable range for the desired requirements.

When the ferrite content data for each weld is taken into account and if the average values of each nine measurements for each position is calculated, a graph as illustrated in Fig. 6a and b can be plotted roughly describing the ferrite and austenite phase distribution of the weld cross sections across the left side of the BM and HAZ, WM, right side of the HAZ and BM.

It is clearly shown that in plasma arc welds, ferrite content of weld metals is higher than the BM (almost 50%) (see Fig. 5). This is because that the weld metal of DSS solidifies primarily as delta ferrite. When it cools down, a partial transformation to austenite initiates at the ferrite grain boundaries and then continues intergranularly. As the weld cools faster, less austenite will be formed in the weld metals as compared to the BM [26].

Combining the impact toughness test results and ferrite content data, Fig. 7a and b can be plotted to determine the ferrite content and impact toughness relationship, respectively, for Weld 1 and Weld 2. Figure 6 includes Charpy impact testing data at subzero temperatures such as −60, −40 and −20 °C.

According to Figs. 5 and 6, it could basically be said that when the ferrite/austenite phase balance is protected, such as close to 50:50%, impact toughness data of WM is improved. When the balance changes, such as 40:60%, low temperature toughness values of WM may show some decrease. Ferrite content depends on the chemical composition of the weld metal and the cooling rates of the weld which are

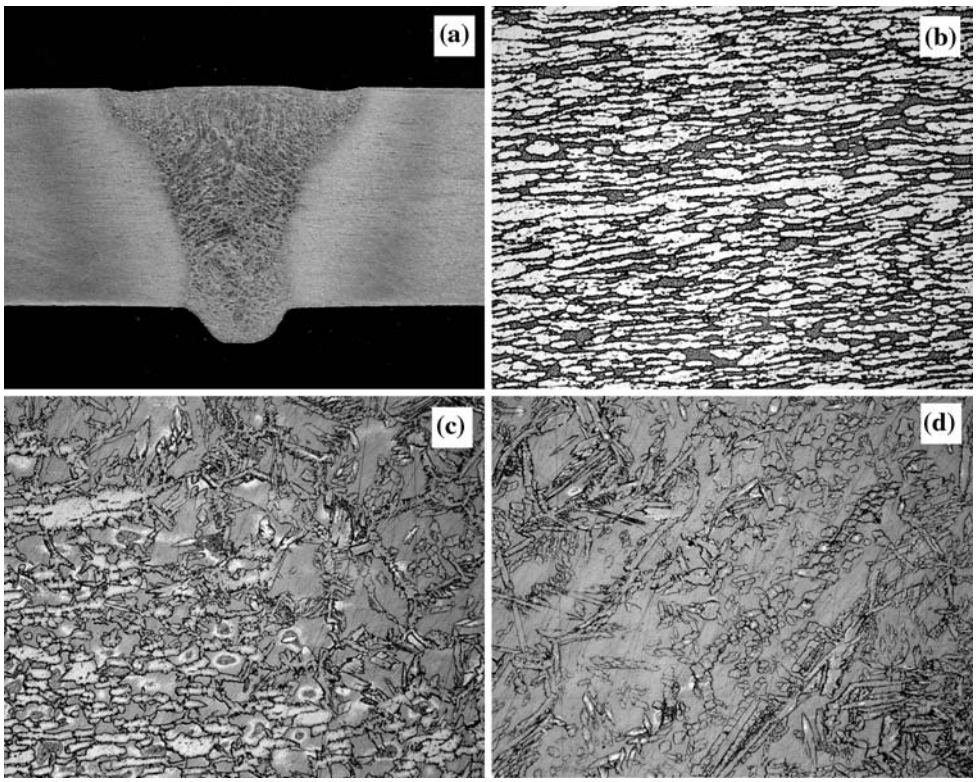

Fig. 3 Macro- and microphotographs of Weld 1: (**a**) macro, (**b**) BM, (**c**) HAZ and (**d**) WM

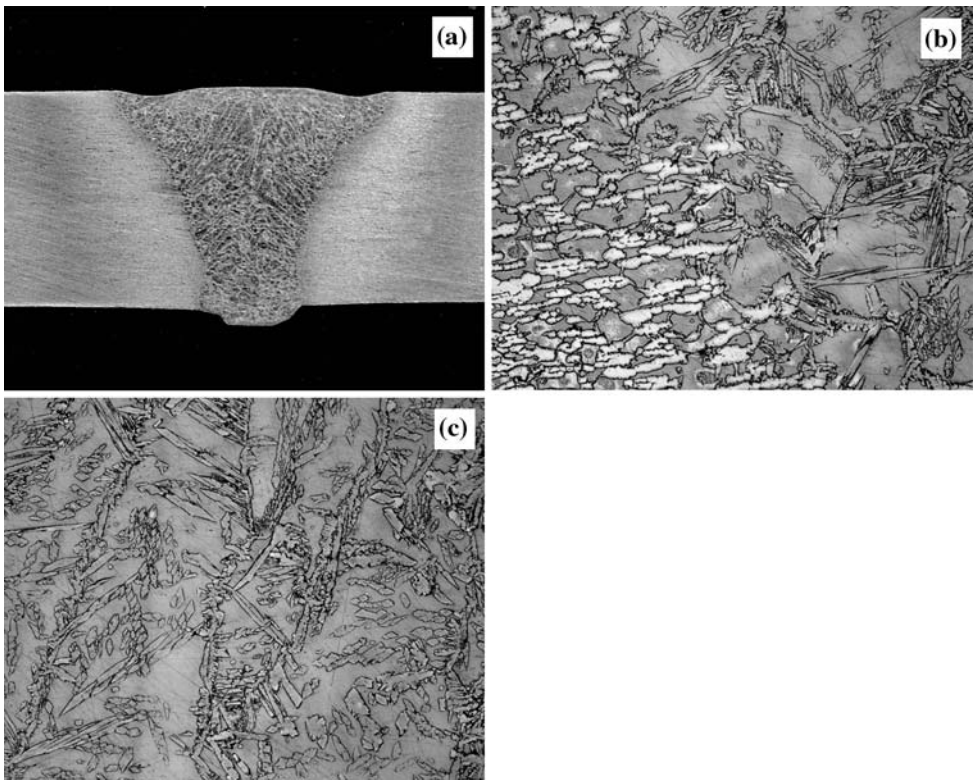

Fig. 4 Macro- and microphotographs of Weld 2: (**a**) macro, (**b**) HAZ and (**c**) WM

related to the heat input during welding [25]. The heat input for the first weld was 1.90 kJ/mm while 2.25 kJ/mm was used for the second weld thereby exceeding the recommended limit of 2 kJ/mm [8, 27]. It would be interesting to compare microstructures and properties of these two welds. During cooling, a transformation from ferrite to

Table 2 Ferrite content analysis of the plasma arc welded joints (in ferrite %)

Position	Weld 1	Weld 2
BM left face	40-41-40/40	38-39-38/38
BM left middle	41-41-40/41	37-37-36/37
BM left root	41-40-40/40	37-37-37/37
HAZ left face	50-50-48/49	46-44-43/44
HAZ left middle	47-45-48/47	44-41-43/43
HAZ left root	49-46-44/46	41-39-41/40
WM face	51-51-54/52	47-48-44/46
WM middle	48-51-49/49	46-44-43/44
WM root	47-46-43/45	43-43-42/43
HAZ right face	47-48-48/48	43-43-44/43
HAZ right middle	49-47-46/47	42-43-40/42
HAZ right root	46-45-45/45	42-41-40/41
BM right face	38-38-37/38	38-39-38/38
BM right middle	36-37-37/37	37-36-37/37
BM right root	37-37-37/37	37-37-37/37

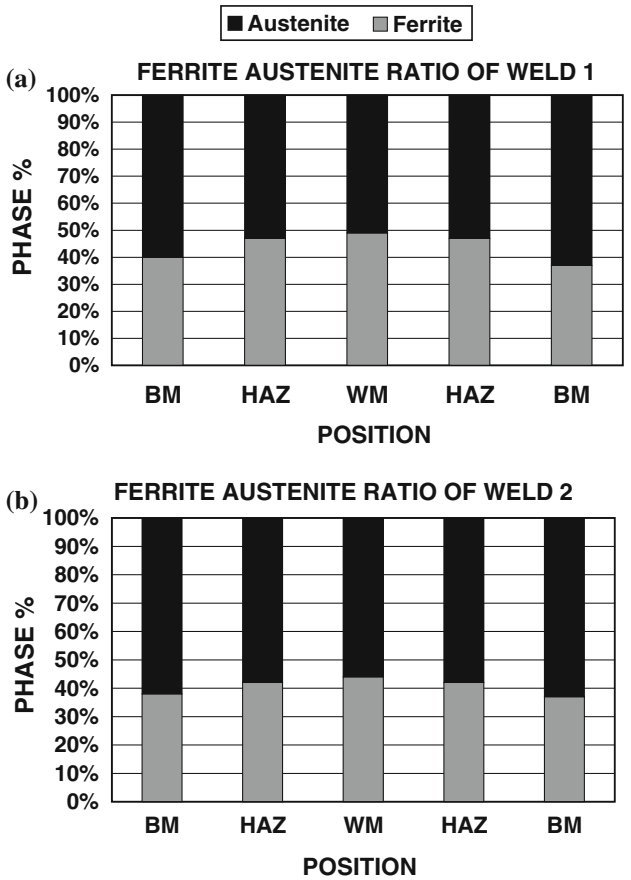

Fig. 5 Ferrite austenite ratio of plasma arc welded joints: (**a**) Weld 1 and (**b**) Weld 2

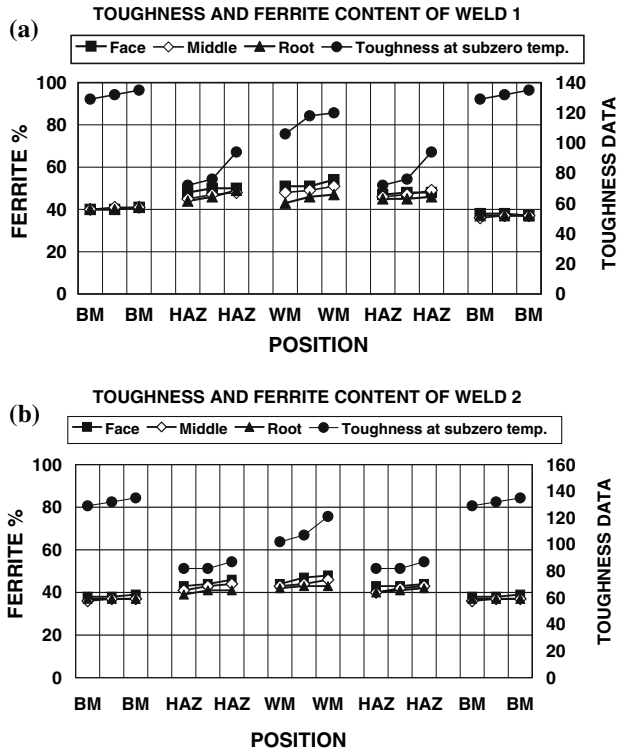

Fig. 6 Toughness and ferrite content relation of the PAW joints: (**a**) Weld 1 and (**b**) Weld 2

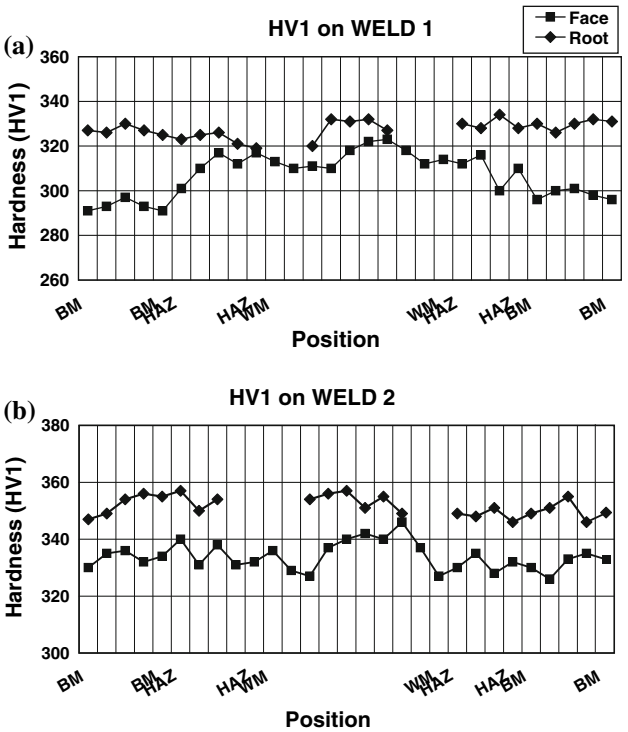

Fig. 7 HV1 graphs of (**a**) Weld 1 and (**b**) Weld 2

austenite occurs so that the elongation of cooling time leads to further transformation progresses such as more austenite formation. Since the cooling time is proportional to the amount of heat input, more ferrite is expected when lower heat input is used [15]. Confirming this situation, ferrite content measurements of welds revealed that less ferrite is

measured on Weld 2 with a heat input of 2.25 kJ/mm with regard to that of Weld 1 with less heat input.

HV1 measurements carried out over the weld cross sections are illustrated in Fig. 7a and b, for Weld 1 and Weld 2, respectively.

For Weld 1, weld metal hardness was between 312 HV1 and 332 HV1. HAZ hardness ranged from 300 HV1 to 334 HV1 while HAZ values ranging from 330 HV1 to 357 HV1 and weld metal values between 327 HV1 and 357 HV1 were measured for Weld 2. Relatively high HAZ hardness data was obtained from Weld 2 which was welded with a higher heat input than Weld 1. There is a few decrease in the ferrite content of Weld 2 resulted with some increase in microhardness. Taking into account of ferrite content measurements of roughly 50 and 45%, respectively, for Weld 1 and Weld 2, it can be concluded that increase at the heat input leads ferrite content of weld metal to decrease and hardness to increase. There is an increased root region hardness for both welds (see Fig. 7), usually due to work hardening caused by deformation induced by shrinkage similar to that in literature [5].

Conclusions

The following conclusions have been drawn concerning the study on PAW of 1.4410 SDSS with different heat inputs.

Defect-free joining of 6.5 mm thick 1.4410 superduplex grade is possible by PAW without filler metal. The promising impact test results showed that both welds have exhibited good WM and HAZ toughness properties at subzero temperatures such as down to −60 °C, compared to the requirements as referred in the literature. Ferrite percentage measurements revealed that the ferrite content varied in an acceptable range depending on the heat input which affects mainly the microstructure such as hardness properties. If good toughness properties are desired, then the phase balance of the weld metal should be kept close to 50:50% ferrite austenite ratio by controlling the heat input range carefully. Increase in the heat input led hardness at the HAZs to increase. As the improved weldability of SDSSs with controlled welding conditions, such as heat input and acceptable ferrite/austenite balance, has been demonstrated leading to higher productivity during welding, PAW which is considered as immature process for superduplex grades, would be largely extended for industrial applications in the near future.

Acknowledgements The author would like to thank colleagues at Industeel, Teknokon Inc., Gedik Welding Inc., Esab AB Sweden, Assan Inc., Cimtas Inc. for their technical support. In addition, Dr. L. Karlsson and Dr. P. Toussaint are acknowledged for the valuable suggestions and technical support.

References

1. Lippold JC, Kotecki DJ (2005) Welding metallurgy and weldability of stainless steels. John Wiley & Sons, NJ
2. Davis JR, Davis & Assoc. (eds) (1994) Stainless steels. American Society for Metals Materials Park, OH
3. Van Nassau L, Meelker H, Hilkes J (1993) Weld World 31, 5:322
4. Karlsson L, Rigdal S, Bergquist EL et al (2007) International conference on Duplex 2007, Italy, paper 11
5. Karlsson L (1999) WRC Bull 438:1 (ISSN 0043-2326)
6. Kaluc E, Taban E (2007) Paslanmaz Celikler, Gelistirilen Yeni Turleri ve Kaynak Edilebilirlikleri. MMO 2007/461, ISBN: 978-9944-89-438-8
7. Karlsson L (1991) Proceedings of international conference on stainless steels, Chiba, p 1093
8. Tavares SSM, Pardal JM, Lima LD et al (2007) Mater Charact 58:610. doi:10.1016/j.matchar.2006.07.006
9. Otarola T, Hollner S, Bennefois B et al (2005) Eng Fail Anal 12:930. doi:10.1016/j.engfailanal.2004.12.022
10. Folkhard E (1988) Welding metallurgy of stainless steels. Springer-Verlag, New York
11. Karlsson L, Tolling J (2006) Proceedings of IIW regional congress on welding and related inspection technologies, South Africa
12. Srinivasan PB, Muthupandi V, Dietzel W et al (2006) J Mater Eng Perform 15(6):758
13. Srinivasan PB, Muthupandi V, Dietzel W et al (2006) Mater Design 27:182. doi:10.1016/j.matdes.2004.10.019
14. McPherson NA, Li Y, Baker TN (2000) Sci Technol Weld Joining 5(4):235
15. Petronius I, Bamberger M (2001) Sci Technol Weld Joining 6(2):79
16. Kordatos JD, Fourlaris G, Papadimitrou G (2001) Scripta Mater 44:401. doi:10.1016/S1359-6462(00)00613-8
17. Muthupandi V, Srinivasan PB, Seshadri SK et al (2003) Mater Sci Eng A358:9. doi:10.1016/S0921-5093(03)00077-7
18. Kuroda T, Ikeuchi K, Ikeda H (2006) Vacuum 80:1331. doi:10.1016/j.vacuum.2006.01.068
19. Ku JS, Ho J, Tjong SC (1997) J Mater Process Technol 63:770. doi:10.1016/S0924-0136(96)02721-5
20. Yip WM, Man HC, Ip WH (1999) Sci Technol Weld Joining 4(4):226
21. Jianxun Z, Qingyan L, Weiwei L et al (2006) Rare Met Mater Eng 35(11):1822
22. Baxter C, Young M (2000) Duplex America conference, stainless steel world. KCI Publishing
23. Comer A, Looney L (2006) Theor Appl Fract Mech 45:139. doi:10.1016/j.tafmec.2006.02.005
24. Sato YS, Nelson TW, Sterling CJ et al (2005) Mater Sci Eng A A397:376. doi:10.1016/j.msea.2005.02.054
25. Urena A, Utero E, Utrilla MV (2007) J Mater Process Technol 182:624. doi:10.1016/j.jmatprotec.2006.08.030
26. Sun Z, Kuo M, Annergren I et al (2003) Mater Sci Eng A356:274. doi:10.1016/S0921-5093(03)00139-4
27. UR47N+ (2007) Product catalogue, Industeel, 8 pp
28. Gooch TG (2000) Corrosion NACE Expo, USA